

see commentary on page 1055

Paricalcitol attenuates cyclosporine-induced kidney injury in rats

Jeong Woo Park¹, Eun Hui Bae¹, In Jin Kim², Seong Kwon Ma¹, Chan Choi³, JongUn Lee² and Soo Wan Kim¹¹Department of Internal Medicine, Chonnam National University Medical School, Gwangju, Korea; ²Department of Physiology, Chonnam National University Medical School, Gwangju, Korea and ³Department of Pathology, Chonnam National University Medical School, Gwangju, Korea

Despite its benefits, the clinical use of cyclosporine A (CsA) is limited by its nephrotoxic properties. Because paricalcitol (19-nor-1,25-hydroxyvitamin D₂) has renoprotective effects, we tested whether it can blunt renal dysfunction and fibrosis in a rat model of CsA-induced nephropathy. Treatment with CsA decreased creatinine clearance, increased monocyte/macrophage infiltration, and increased the expression of inflammatory cytokines within the kidney. Paricalcitol reduced the decline in kidney function and pro-fibrotic changes and also blunted the increased transforming growth factor (TGF)- β 1 expression and Smad signaling. Using an *in vitro* model, we treated HK-2 cells with CsA and found that paricalcitol attenuated the CsA-induced increases in phosphorylated extracellular signal-regulated and c-Jun N-terminal kinases, and also prevented the activation of nuclear factor- κ B. Paricalcitol effectively prevented TGF- β 1-induced epithelial-to-mesenchymal transitions and extracellular matrix accumulation as evidenced by attenuated collagen deposition and fibrosis in CsA-treated rats. In addition, paricalcitol decreased the number of TUNEL-positive nuclei and reduced the expression of pro-apoptotic markers in CsA-treated HK-2 cells. Thus, paricalcitol appears to attenuate CsA-induced nephropathy by suppression of inflammatory, pro-fibrotic, and apoptotic factors through inhibition of the nuclear factor- κ B, Smad, and mitogen-activated protein kinase signaling pathways.

Kidney International (2010) **77**, 1076–1085; doi:10.1038/ki.2010.69; published online 17 March 2010

KEYWORDS: cyclosporine; fibrosis; inflammation; paricalcitol

Deficiency in vitamin D and its active metabolites is a common pathological feature in chronic kidney disease. In addition to its primary role in calcium homeostasis and bone mineralization, vitamin D is known to have an important function in cellular homeostasis, including hormone secretion, cell proliferation, and differentiation. Many previous studies have focused on the effects of calcitriol, an active form of vitamin D, or its analogs on glomerular damage,^{1–3} whereas kidney tubules, including the proximal tubule, have been identified as another target of active vitamin D.^{4,5} The suppressive effect of calcitriol on renal interstitial myofibroblasts indicates that calcitriol inhibits the development of renal interstitial fibrosis.⁶ Paricalcitol (19-nor-1,25-dihydroxyvitamin D₂) is an active, nonhypercalcemic vitamin D analog that shows similar biological activity, but has fewer adverse effects and increased tolerance.⁷ Recently, several investigators postulated that paricalcitol is renoprotective in various experimental nephropathy models through its anti-inflammatory and anti-fibrotic actions.^{8–10}

Cyclosporine A (CsA) is used to prevent rejection in various types of organ transplantation and in the treatment of many autoimmune diseases. Despite its clinical benefits, the clinical use of CsA is limited by its nephrotoxic potential. However, the mechanism for CsA-induced nephropathy (CIN) is still incompletely understood and the molecular basis remains undefined. CIN causes an irreversible decline in renal function, which is characterized by both renal vasoconstriction and structural damage, including arteriolar hyalinosis, tubular atrophy, interstitial fibrosis, and glomerular sclerosis.^{11,12} It has been known that CsA leads to activation of the intrarenal renin-angiotensin system, which reduces renal blood flow through the action of angiotensin II. Angiotensin II has pleiotropic effects, including aldosterone release, stimulation of tubular transport, pro-inflammatory effects, and fibrogenic stimulatory actions, which are mediated by transforming growth factor (TGF)- β signaling. Local renal hypoxia or ischemia resulting from renal vasoconstriction led to the production of reactive oxygen species that caused cellular injury and promoted cell death by apoptosis.¹³ CsA also directly activates apoptotic genes and increases apoptosis in tubular and interstitial cells, resulting

Correspondence: Soo Wan Kim, Department of Internal Medicine, Chonnam National University Medical School, Hakdong 8, Donggu, Gwangju 501-757, Korea. E-mail: skimw@chonnam.ac.kr

Received 21 September 2009; revised 6 January 2010; accepted 19 January 2010; published online 17 March 2010

in tubular atrophy. In addition, inflammatory changes, such as macrophage infiltration into the damaged kidney, are associated with chronic CIN.¹⁴

TGF- β has a pivotal function in progressive renal disease, including CIN. Importantly, CsA directly upregulates TGF- β expression in tubular epithelial cells, independently of the hemodynamic effects of the renin-angiotensin system in chronic CIN.^{15,16} TGF- β promotes renal fibrosis by increasing the production and decreasing the degradation of extracellular matrix (ECM) components in the damaged kidney. In addition, the inhibition of TGF- β using anti-TGF- β antibodies reduced tubular epithelial apoptosis and decreased the extent of tubular atrophy in an experimental model.¹⁷ These observations suggest that, beyond its effects on ECM accumulation, TGF- β signaling may initiate renal tubular cell pro-apoptotic effectors and the epithelial-to-mesenchymal transition (EMT) in tubular epithelial cells, resulting in tubular degeneration and tubular atrophy.

This study investigated the effect of paricalcitol on the progression of CIN. To elucidate its mechanism of action, we examined the effect of paricalcitol on renal inflammation, apoptosis, fibrosis, and tubular epithelial integrity after CsA-induced injury.

RESULTS

Functional parameters

Table 1 shows changes in functional parameters as a result of CsA treatment. In rats, CsA increased plasma creatinine levels and decreased creatinine clearance rate compared to controls. Urine osmolality also decreased in the CsA-treated group compared to controls. Urine albumin excretion increased with CsA compared to controls. In contrast, paricalcitol co-treatment attenuated the negative effects of CsA. The mean blood CsA level was not significantly altered with paricalcitol co-treatment.

Effects of paricalcitol on morphological changes in CIN

Figure 1 shows morphological change among three groups. Hematoxylin and eosin staining revealed variable sizes of tubular vacuolization, tubular atrophy associated with cystic dilation in the proximal tubules in CsA-treated

rats compared with those in controls. Sparse interstitial infiltration of mononuclear cells and widening of interstitial spaces are also shown in CsA-treated rats. Paricalcitol ameliorated these changes. Vimentin and Masson's trichrome staining confirmed that CsA induced collagen deposition and fibrosis in the kidney, which were ameliorated by paricalcitol (Figure 1a). Tubulointerstitial damage score and staining for Masson's trichrome significantly increased in CsA-treated rats, which were attenuated by paricalcitol (Figure 1b).

Effects of paricalcitol on inflammatory cell infiltration, inflammatory cytokines, and adhesion molecules in CIN

To determine the effects of paricalcitol on renal inflammatory cell infiltration, we analyzed ED-1 protein expression and the infiltration of ED-1-positive macrophages in renal tissue. ED-1 expression in the cortex/outer stripe of the outer medulla (OSOM) increased significantly in CsA-treated rats compared to controls; paricalcitol attenuated increased ED-1 expression (Figure 2a). Similarly, paricalcitol co-treatment abrogated the significant increase of ED-1-positive macrophages infiltration in CsA-treated animals (Figure 2b). The expression of inducible nitric oxide synthase (iNOS), which is synthesized during inflammation in renal disease, increased in cortex/OSOM from CsA-treated rats compared to controls, which was reversed by paricalcitol (Figure 2c).

We also investigated the expression of tumor necrosis factor- α , interferon- γ , and interleukin-1 β , which are key inflammatory cytokines produced by infiltrating cells. As shown in Figure 3, CsA significantly induced renal tumor necrosis factor- α , interleukin-1 β , and interferon- γ mRNA expression; paricalcitol co-treatment attenuated these effects. Certain chemokines and adhesion molecules, such as monocyte chemoattractant protein-1, intercellular adhesion molecule-1, and vascular cell adhesion molecule-1, which activate or recruit the transmigration of inflammatory cells into the site of renal injury, were also shown. CsA induced the expression of these factors, which was also attenuated by paricalcitol co-treatment.

Effects of paricalcitol on NF- κ B expression in CIN

Nuclear factor- κ B (NF- κ B) is released from an inhibitory subunit I κ B and translocates into the nucleus, where it promotes the transcriptional activation of target genes. We assessed the effect of CsA (20 μ mol/l) and paricalcitol on the expression of phosphorylated NF- κ B p65 subunit (P-p65) in nuclear extracts and total I κ B- α in cytoplasm of renal proximal tubular epithelial cell line (HK-2). The nuclear translocation of p65 subunits began to increase at 15 min, peaked at 30 min after CsA exposure, and diminished progressively afterward (Figure 4a). Cytoplasmic total I κ B- α expression was not changed in CsA-treated cells. P-p65 expression was also examined in HK-2 cells, which were pretreated with paricalcitol (0.2 ng/ml) for 3 h followed by CsA (20 μ mol/l) exposure for 30 min. The expression of P-p65 was increased in CsA-treated cells compared to untreated controls, whereas paricalcitol pretreatment

Table 1 | Changes in renal functional parameters

	Control	CsA	CsA+Pari
<i>n</i>	8	8	10
P _{Cr} (mg/dl)	0.4 ± 0.0	0.9 ± 0.1**	0.6 ± 0.1 [‡]
C _{Cr} (ml/min)	2.4 ± 0.4	0.6 ± 0.1*	1.2 ± 0.2 [‡]
U _{Osm} (mOsm/kg H ₂ O)	1294.0 ± 49.2	534.4 ± 18.1**	871.3 ± 107.5 [‡]
UAE (mg/g Cr)	4.3 ± 0.5	12.7 ± 1.1**	2.9 ± 1.8 [‡]
CsA concentration (ng/ml)	NM	2467.0 ± 66.7	2376.0 ± 31.4

Abbreviations: C_{Cr}, creatinine clearance; CsA, cyclosporine; *n*, number of rats; NM, not measured; P_{Cr}, plasma creatinine; Pari, paricalcitol; U_{Osm}, urine osmolality; UAE, urine albumin excretion.

P* < 0.05; *P* < 0.01 compared with control. [‡]*P* < 0.05; [‡]*P* < 0.01 compared with CsA-treated rats.

Values are expressed as the mean ± s.e.m.

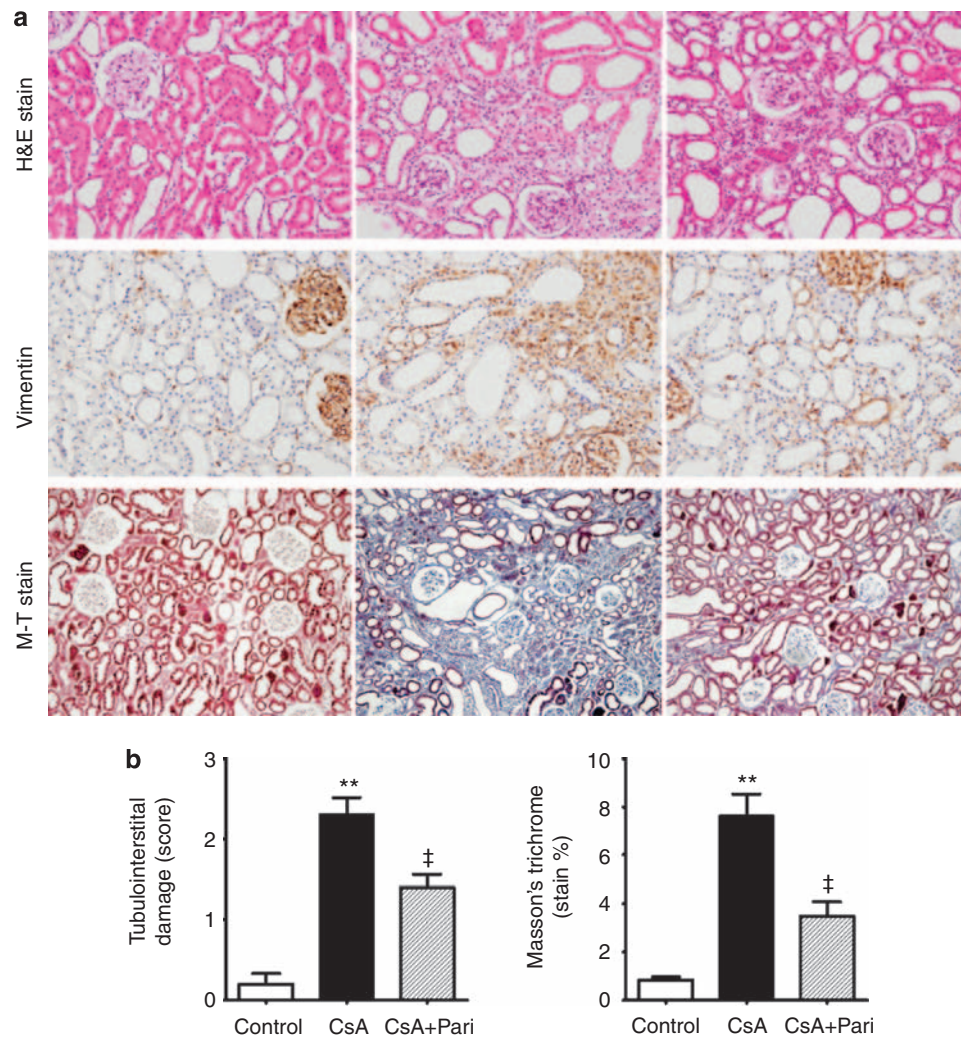


Figure 1 | Representative microscopic findings (original magnification, $\times 200$). (a) Hematoxylin and eosin (H&E), vimentin, and Masson's trichrome (M-T) staining in rat kidneys. (b) Staining was quantified by image analysis. In H&E stain, tubular vacuolization and atrophy were associated with dilation in the proximal tubules in CsA-treated rats compared with those in controls. Note the sparse interstitial infiltration of mononuclear cells and widening of interstitial spaces also shown in CsA-treated rats. Paricalcitol ameliorated these changes. Vimentin, a marker of actin microfilament and Masson's trichrome staining, confirmed that CsA treatment increased collagen deposition and fibrosis in the kidney, which were ameliorated by paricalcitol co-treatment. CsA, cyclosporine; Pari, paricalcitol. Each column represents the mean \pm s.e.m. ($n = 5$). ** $P < 0.01$ compared to the control. ‡ $P < 0.01$ compared to CsA-treated rats.

prevented this increase. Total I κ B- α expression was equivalent among three groups (Figure 4b).

Effects of paricalcitol on TGF- β 1 and Smad signaling in CIN

Semiquantitative immunoblotting revealed that the expression of TGF- β 1, an important pro-fibrotic molecule derived from infiltrating inflammatory cells, increased significantly in the cortex/OSOM of CsA-treated rats, and this effect was markedly attenuated by paricalcitol. We also assessed the TGF- β 1-triggered Smad signaling pathway by evaluating the total Smad-2/3 and Smad-4 levels and the level of inhibitory Smad-6. An increase in total Smad-2/3 in CIN was accompanied by an increase in Smad-4 content and a decrease in inhibitory Smad-6 compared to the control group. These CsA-induced changes were again restored by paricalcitol co-treatment (Figure 5).

Effects of paricalcitol on ERK 1/2 and JNK expression in CIN

In HK-2 cells, CsA treatment (20 μ mol/l) increased the levels of phosphorylated extracellular signal-regulated kinase (pERK) 1/2 compared to the control. In contrast, pretreatment with paricalcitol (0.2 ng/ml) for 3 h before CsA administration suppressed CsA-induced pERK overexpression. Phosphorylated c-Jun N-terminal kinase (pJNK) expression also increased in HK-2 cells incubated with CsA, and this effect was reversed by paricalcitol pretreatment (Figure 6).

Effects of paricalcitol on EMT in CIN

We next examined the expression of the epithelial receptor E-cadherin and α -smooth muscle actin (SMA), a molecular marker of myofibroblasts. Figure 7 shows that paricalcitol maintained E-cadherin expression and inhibited the

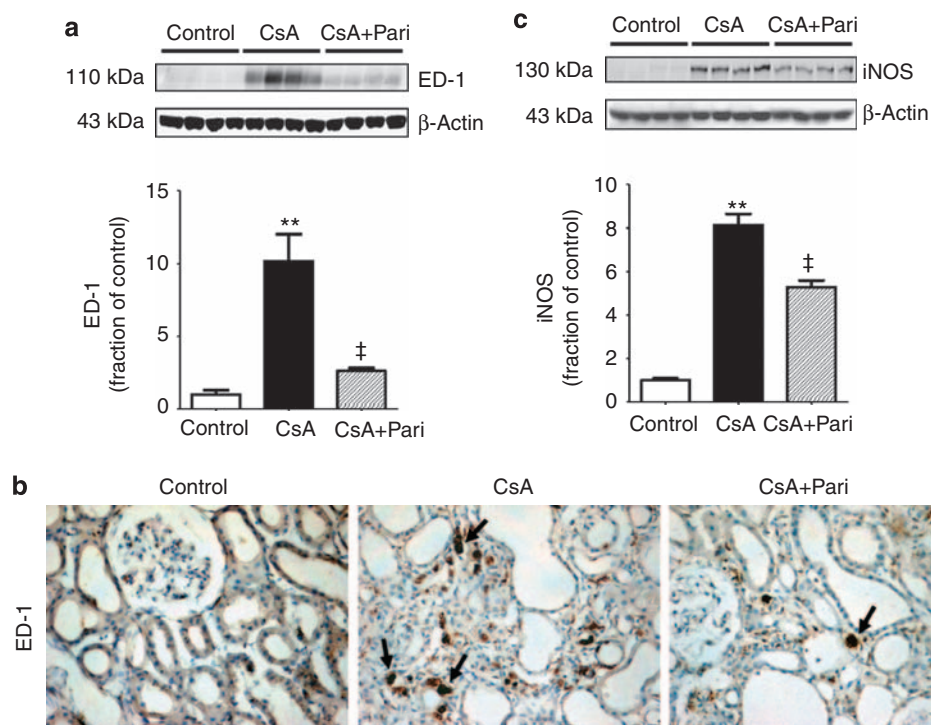


Figure 2 | Effects of paricalcitol on inflammatory cell infiltration and inducible nitric oxide synthase (iNOS) expression.

(a) Semiquantitative immunoblotting of ED-1 expression. Inflammatory cell infiltration was determined by immunohistochemical staining for ED-1, a specific marker of macrophages, in the cortex/outer stripe of the outer medulla (OSOM). (b) The infiltration of ED-1-expressing cells increased significantly in CsA-treated rats, which was ameliorated by paricalcitol treatment (original magnification, $\times 200$). Arrows indicate infiltrated ED-1-positive cells. (c) Semiquantitative immunoblotting of iNOS in cortex/OSOM. The expression of iNOS increased during CsA challenge, compared to the control, and was counteracted by paricalcitol co-treatment. Each column represents the mean \pm s.e.m. ($n = 8$). ** $P < 0.01$ compared to the control. ‡ $P < 0.01$ compared to CsA-treated rats. CsA, cyclosporine; Pari, paricalcitol.

induction of α -SMA in CsA-treated rats, consistent with the observed changes in TGF- β 1 expression. In HK-2 cells, CsA increased fibronectin and connective tissue growth factor (CTGF) expression compared to the control, and this effect was inhibited by paricalcitol pretreatment (Figure 8).

Effects of paricalcitol on renal tubular cell apoptosis in CIN

To determine the protective effects of paricalcitol on CsA-induced renal tubular apoptosis, we performed terminal deoxynucleotidyl transferase-mediated dUTP nick-end labeling (TUNEL). The number of tubular epithelial cells containing TUNEL-positive nuclei increased in CsA-treated rat kidney; paricalcitol co-treatment attenuated this effect (Figure 9). Furthermore, CsA induced increases in pro-apoptotic markers, such as Bax and total and cleaved caspase-3 levels, which were attenuated by paricalcitol in HK-2 cells. In contrast, the expression of anti-apoptotic protein Bcl-2 was decreased in renal tubular cells incubated with CsA, which was also attenuated by paricalcitol (Figure 10).

Effects of paricalcitol on rat kidney and HK-2 cells

To ascertain the proper effects of paricalcitol on rat kidney and HK-2 cells, we performed an experiment for another set of rats and HK-2 cells, which were administered vehicle or buffer alone and paricalcitol alone. When comparing control

to paricalcitol group, there was no significant difference in renal functional parameters (Supplementary Table S1). The expression of inflammatory cytokines (Supplementary Figure S1), P-p65, total I κ B- α , and TGF- β 1 was not altered with paricalcitol. We also assessed the expression of mitogen-activated protein kinases (MAPKs), EMT markers, apoptotic markers, and anti-apoptotic markers in HK-2 cells, which was not changed by paricalcitol (Supplementary Figure S2).

DISCUSSION

The infiltration of inflammatory cells into the interstitium is a prominent pathological finding in progressive renal disease, and these infiltrating inflammatory cells are important sources of pro-fibrotic molecules, including TGF- β 1.^{18,19} Chemokines and adhesion molecules are also activated, hence recruit and induce the transmigration of inflammatory cells into sites of renal injury. In this study, we showed that paricalcitol reduced the CsA-induced increases in the levels of chemokines, iNOS and adhesion molecules, and ED-1-positive monocyte/macrophage infiltration, suggesting that paricalcitol has an anti-inflammatory function.

Recent studies in CIN model, in which free radicals induced oxidative stress, lead to the upregulation of iNOS and NF- κ B expression in response to CsA. In their studies, chemical blockade using antioxidants reduced iNOS and

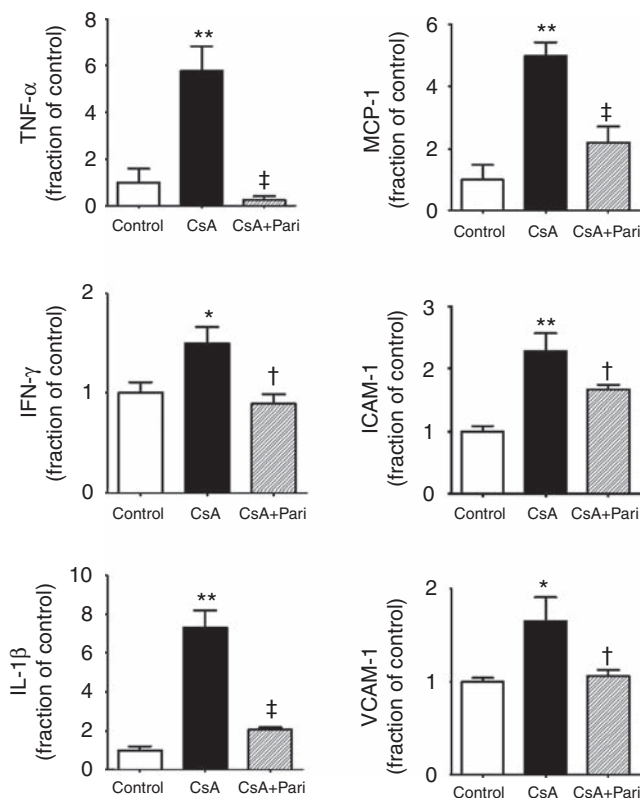


Figure 3 | Effects of paricalcitol on inflammatory cytokines and adhesion molecules. Real-time polymerase chain reaction (PCR) was used to examine the expression of tumor necrosis factor (TNF)- α , interferon (IFN)- γ , and interleukin (IL)-1 β , which are pro-inflammatory cytokines that participate in the pathogenesis of renal disease. Chemoattractants and adhesion molecules, such as monocyte chemoattractant protein (MCP)-1, intercellular adhesion molecule (ICAM)-1, and vascular cell adhesion molecule (VCAM)-1, were also evaluated. These inflammatory cytokines are significantly elevated in CsA-treated rats compared to those in control rats. Paricalcitol co-treatment suppressed the CsA-induced overexpression of these inflammatory cytokines and adhesion molecules. Each column represents the mean \pm s.e.m. ($n = 8$). * $P < 0.05$ and ** $P < 0.01$ compared to the control. † $P < 0.05$ and ‡ $P < 0.01$ compared to CsA-treated rats. CsA, cyclosporine; Pari, paricalcitol.

NF- κ B overexpression.^{20,21} We also found that CsA increases renal iNOS expression and nuclear translocation of p65 NF- κ B subunit. Paricalcitol attenuated these changes, suggesting that vitamin D exerts its immunomodulatory effects in CIN through the regulation of NF- κ B and NO signaling. The mean blood CsA concentration was not changed with paricalcitol co-treatment; hence, the beneficial effect of paricalcitol on CIN was not attributed to the less CsA exposition in rats.

TGF- β is a key molecule in renal disease progression. Beyond its effect on ECM accumulation, TGF- β signaling initiates renal tubular cell pro-apoptotic effectors and EMT in tubular epithelial cells, resulting in tubular degeneration and tubular atrophy. EMT is a process in which renal tubular cells lose their epithelial phenotype and acquire new features of the mesenchyme. We showed that TGF- β 1 expression was

increased in CsA-treated rats, which was ameliorated by paricalcitol co-treatment. TGF- β 1 signals are transduced by transmembrane serine/threonine kinase type I and type II receptors and intracellular mediators known as Smads. On TGF- β 1 stimulation, receptor-bound Smad proteins, such as Smad-2/3, are phosphorylated. Phosphorylation induces the association of Smad-2/3 with Smad-4, a member of the co-Smad subfamily, and they form transcriptionally active complexes that translocate into the nucleus and activate the transcription of TGF- β -induced target genes, including CTGF. Smad signaling can also be negatively controlled by the inhibitory Smad-6 and Smad-7 proteins. For these reasons, TGF- β 1-induced EMT is thought to be mediated by Smad signaling.^{22,23} In this study, CsA induced the overexpression of Smad-2/3 and Smad-4, whereas inhibitory Smad-6 expression was decreased in response to CsA. Importantly, paricalcitol effectively reversed these effects. In addition, paricalcitol preserved E-cadherin expression and inhibited α -SMA induction in CsA-induced renal injury. This suggests that paricalcitol may specifically target tubular EMT, a key event in the pathogenesis of renal interstitial fibrosis.

CsA also modulated the expression of MAPKs. Specifically, CsA-induced ERK 1/2 and c-JNK phosphorylation in rat kidney, and these increases were attenuated by paricalcitol. In addition to Smad signaling, a comprehensive survey indicated that TGF- β 1 is capable of activating several other signal transduction pathways in tubular epithelial cells, such as MAPKs.²⁴ TGF- β 1 activates the ERK and JNK pathways, and accumulating evidence suggests a function for these signaling pathways in CIN. For example, ERK and PI3K signaling may be involved in CsA-induced reactive oxygen species generation and subsequent renal cell damage.²⁵ Other groups have also suggested that the activation of ERK signaling has a critical function in the proliferation of tubular epithelial and myofibroblast-like cells.²⁶ JNK signaling is also involved in TGF- β 1-induced fibronectin and CTGF production²⁷ and interstitial myofibroblast accumulation²⁸ suggesting a function for JNK in renal fibrogenesis. In this study, we showed that paricalcitol reduced ERK 1/2 and c-JNK activation in CsA-treated rat kidneys. These changes coincided with the expression of EMT markers, such as E-cadherin and α -SMA, *in vivo* and the expression of CTGF and fibronectin in HK-2 cells. Therefore, ERK 1/2 and c-JNK signaling pathways activated by TGF- β 1 appear to mediate CsA-induced renal fibrosis, which is effectively inhibited by paricalcitol. Masson's trichrome staining confirmed the paricalcitol-induced attenuation of collagen deposition and fibrosis in CIN.

In progressive renal disease, tubular cell apoptosis precedes manifestations of tubular atrophy, tubular dilatation, and perivascular inflammation.²³ Yang *et al.*²⁹ also showed that loss of cellularity progresses over time together with the activation of apoptosis-related gene expression until fibrotic tissue replaces the apoptotic cells in a chronic CIN model. Accordingly, CsA induces Bax aggregation and

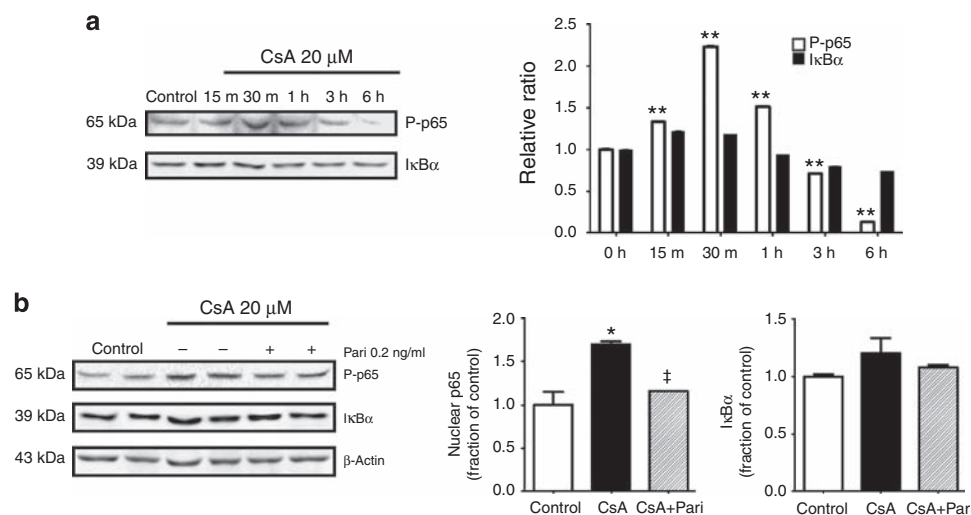


Figure 4 | *In vitro* analysis of the phosphorylated nuclear factor- κ B (NF- κ B) p65 subunit and total I κ B- α expression in HK-2 cells. (a) Semiquantitative immunoblotting at various time points after treatment with CsA (20 μ mol/l). The open bars indicate that the expression of phosphorylated p65 subunit (P-p65) increased significantly compared to the control, beginning at 15 min after treatment and peaking at 30 min. Cytoplasmic total I κ B- α expression was not significantly changed in CsA-treated cells compared to control cells. (b) In contrast, pretreatment with paricalcitol (0.2 ng/ml) for 3 h before exposure to CsA (20 μ mol/l) for 30 min suppressed the overexpression of P-p65 in HK-2 cells. Total I κ B- α expression was equivalent among control and CsA HK-2 cells with or without paricalcitol treatment. Each column represents the mean \pm s.e.m. of three independent experiments performed in duplicate at each time point. * P <0.05 and ** P <0.01 compared to the control. ‡ P <0.01 compared to CsA-treated HK-2 cells. CsA, cyclosporine; Pari, paricalcitol.

translocation to the mitochondria, causing activation of caspase-9, which then cleaves and activates the effector caspase, caspase-3, leading to a loss of mitochondrial transmembrane potential and apoptotic cell death.³⁰ In this study, the number of TUNEL-positive cells increased after CsA treatment. Along with these changes, CsA increased the expression of Bax protein and cleaved caspase-3, whereas it downregulated expression of the anti-apoptotic protein Bcl-2. These changes were reversed by paricalcitol, confirming that paricalcitol prevents apoptosis and tubular atrophy, likely through the inhibition of TGF- β 1 expression.

In conclusion, the active vitamin D analog paricalcitol exerts anti-inflammatory effects through the inhibition of NF- κ B and NO signaling, resulting in a reduction of TGF- β 1 expression and TGF- β 1-induced Smad-2/3 and MAPK signaling in chronic CIN. This inhibition of TGF- β 1 signaling appears to attenuate CsA-induced renal tubular cell apoptosis and fibrosis. Although further clinical randomized study of paricalcitol as a possible renoprotective agent in CIN is warranted, our observation provides good evidence that paricalcitol has significant potential as a therapeutic intervention for CIN.

MATERIALS AND METHODS

Animals

The experimental protocol was approved by the Institutional Animal Care and Use Committee of Chonnam National University Medical School. Male Sprague–Dawley rats weighing 180–200 g were allowed *ad libitum* access to a low-salt diet (0.05% sodium; Teklad Premier, Madison, WI, USA) and tap water. CsA (Novartis Pharma, Basel, Switzerland) was dissolved in olive oil (Sigma Chemical,

St Louis, MO, USA) to 20 mg/ml. Three groups of rats were injected with vehicle alone ($n=8$), CsA alone ($n=10$, 20 mg/kg/day, s.c.) and CsA plus paricalcitol (0.2 μ g/kg/day, s.c.; Abbott Laboratories, North Chicago, IL, USA) (CsA + Pari, $n=10$). Another set of rats was injected with vehicle alone ($n=8$) and paricalcitol alone ($n=8$, 0.2 μ g/kg/day, s.c.) for 28 days to ascertain the proper effect of paricalcitol in rat kidney. CsA rats showed 20% mortality rate, whereas all of the controls and CsA + Pari rats were survived during the experiments. Rats were maintained in individual metabolic cages for the last 3 days of the experiment to allow urine collection. On the day of the experiment, we anesthetized the rats with isoflurane. Blood samples were collected from the inferior vena cava. The right kidney was removed rapidly, dissected into the cortex/OSOM, and processed for semiquantitative immunoblotting as described below. The left kidney was fixed through retrograde perfusion for immunohistochemistry. Another series of experiment was conducted for the assay of real-time polymerase chain reaction (PCR). The rats were decapitated under a conscious state, and their kidneys were taken and kept at -70°C until assayed for the mRNA expression by real-time PCR.

Cell culture and application of CsA and paricalcitol to HK-2 cells

To investigate the underlying molecular mechanisms of CsA-induced tubule cell injury, we examined the NF- κ B, MAPKs, and EMT fibrosis and apoptotic factors in HK-2 cells. HK-2 cells were purchased from the American Type Culture Collection (ATCC, Manassas, VA, USA) and cultured. Briefly, cells were passaged every 3–4 days in 100-mm dishes using Dulbecco's modified Eagle's medium-F12 (Sigma Chemical) supplemented with 10% fetal bovine serum (Life Technologies, Gaithersburg, MD, USA), 100 U/ml penicillin, and 100 mg/ml streptomycin (Sigma Chemical). These cells were incubated in a humidified atmosphere

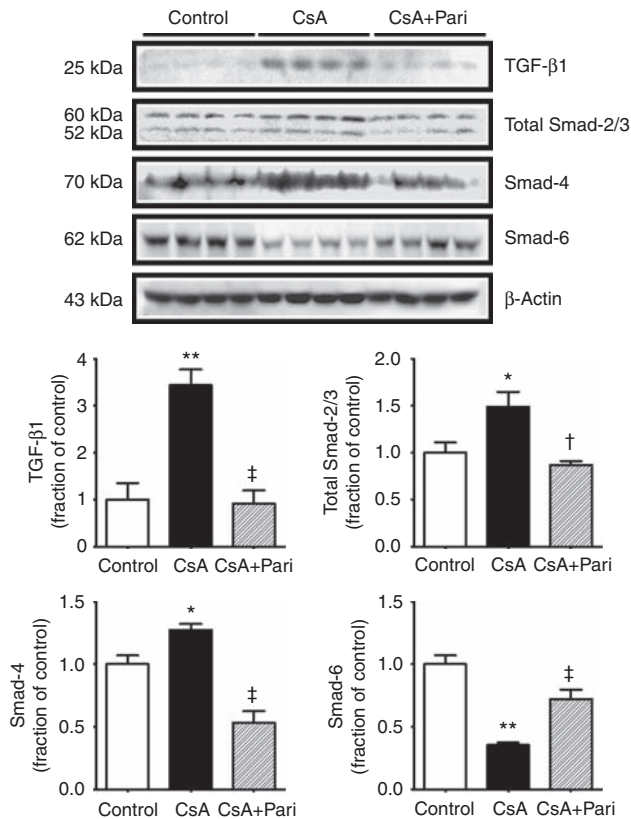


Figure 5 | Effects of paricalcitol on transforming growth factor (TGF)-β1 expression and Smad proteins in CsA-induced renal injury. Semiquantitative immunoblotting for TGF-β1 and Smad-2/3, Smad-4, and Smad-6 proteins. TGF-β1 expression increased significantly in cortex/outer stripe of the outer medulla (OSOM) of CsA-treated rats, which was markedly attenuated by paricalcitol co-treatment. Consistent with the changes in TGF-β1, increases in Smad-2/3 and Smad-4 protein expression suggest that TGF-β1 triggered the Smad signaling cascade. The expression of inhibitory Smad-6 decreased in CsA-treated rats compared to the control group. These CsA-induced changes were inhibited by paricalcitol co-treatment. Each column represents the mean ± s.e.m. (*n* = 8). **P* < 0.05 and ***P* < 0.01 compared to the control. †*P* < 0.05 and ‡*P* < 0.01 compared to CsA-treated rats. CsA, cyclosporine; Pari, paricalcitol.

of 5% CO₂, 95% air at 37 °C for 24 h and subcultured at 70–80% confluence. For experimental use, we plated HK-2 cells onto 60-mm dishes in medium containing 10% fetal bovine serum for 24 h and then switched cells to Dulbecco’s modified Eagle’s medium-F12 with 2% fetal bovine serum for 16 h. These cells were treated with CsA (10 or 20 μmol/l) in the presence or absence of paricalcitol (0.2 ng/ml). Another set of HK-2 cells was treated with paricalcitol alone (0.2 ng/ml) to ascertain the proper effect of paricalcitol in HK-2 cells. Control cells received buffer only, instead of CsA or paricalcitol. The cells were harvested at the end of the treatment for further analysis.

Histological examination

A perfusion needle was inserted into the abdominal aorta and the vena cava was cut to establish an outlet. Blood was flushed from the kidney with cold phosphate-buffered saline (PBS; pH 7.4) for

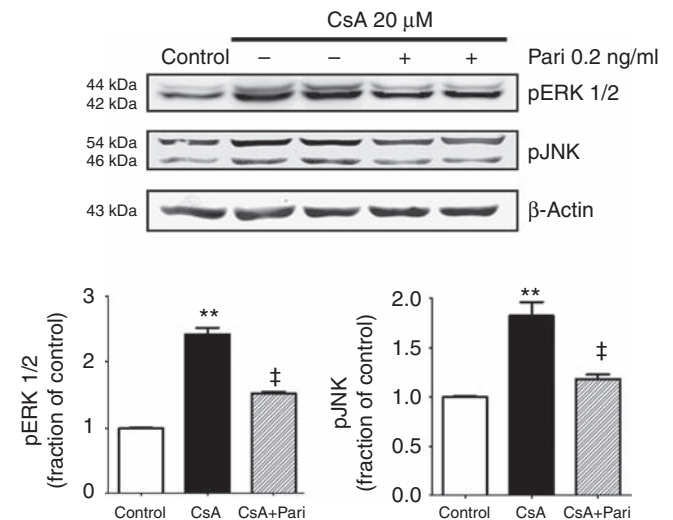


Figure 6 | Effects of paricalcitol on the phosphorylation of extracellular signal-regulated kinase (pERK 1/2) and c-Jun N-terminal kinase (pJNK) in HK-2 cells. HK-2 cells were pretreated with paricalcitol (0.2 ng/ml) for 3 h before incubation with CsA (20 μmol/l) for 1 h. CsA treatment increased the levels of pERK 1/2 and pJNK, whereas paricalcitol pretreatment suppressed these effects. Each column represents the mean ± s.e.m. of three independent experiments performed in duplicate at each time point. ***P* < 0.01 compared to the control. †*P* < 0.01 compared to CsA-treated HK-2 cells. CsA, cyclosporine; Pari, paricalcitol.

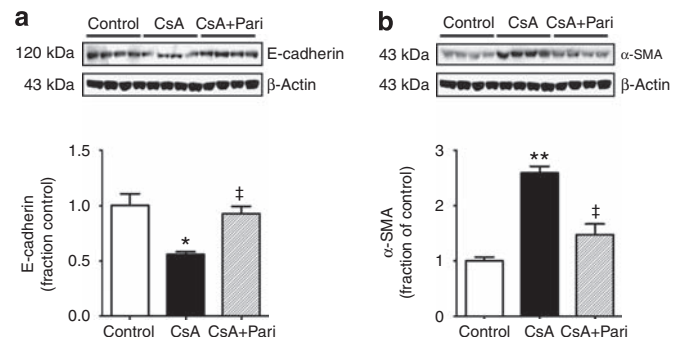


Figure 7 | Effects of paricalcitol on the epithelial-to-mesenchymal transition (EMT). Semiquantitative immunoblotting revealed that CsA treatment significantly decreased the expression of epithelial adhesion receptor E-cadherin (a) and increased that of α-smooth muscle actin (SMA), a molecular marker of myofibroblasts (b), consistent with tubular EMT. In contrast, paricalcitol treatment attenuated these effects, likely through the suppression of CsA-induced transforming growth factor (TGF-β1) signaling. Each column represents the mean ± s.e.m. (*n* = 8). **P* < 0.05 and ***P* < 0.01 compared to the control. †*P* < 0.01 compared to CsA-treated rats. CsA, cyclosporine; Pari, paricalcitol.

15 s before switching to cold 3% paraformaldehyde in 0.1 mol/l cacodylate buffer (pH 7.4) for 3 min. The kidney was removed and cut into transverse sections 2–3 mm thick, which were immersion fixed for 1 h, followed by three 10-min washes in 0.1 mol/l cacodylate buffer, pH 7.4. The tissue was dehydrated in a graded ethanol series and left overnight in xylene. After embedding in paraffin, we cut sections 2 μm thick on a rotary microtome (Leica Microsystems, Herlev, Denmark). Hematoxylin and eosin staining was performed to

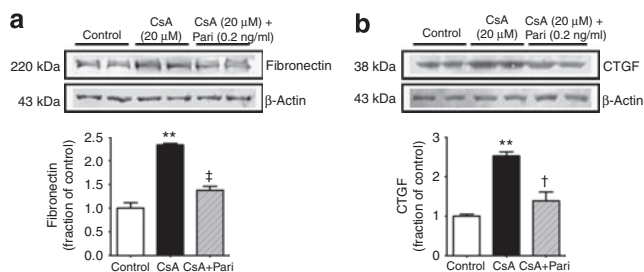


Figure 8 | Effects of paricalcitol on the expression of fibronectin and connective tissue growth factor (CTGF). Semiquantitative immunoblotting of (a) fibronectin and (b) CTGF expression in HK-2 cells incubated with CsA (20 μmol/l) in the absence or presence of paricalcitol (0.2 ng/ml). CsA, cyclosporine; Pari, paricalcitol. Each column represents the mean ± s.e.m. of three independent experiments performed in duplicate. ***P* < 0.01 compared to the control. †*P* < 0.05 and ‡*P* < 0.01 compared to CsA-treated HK-2 cells.

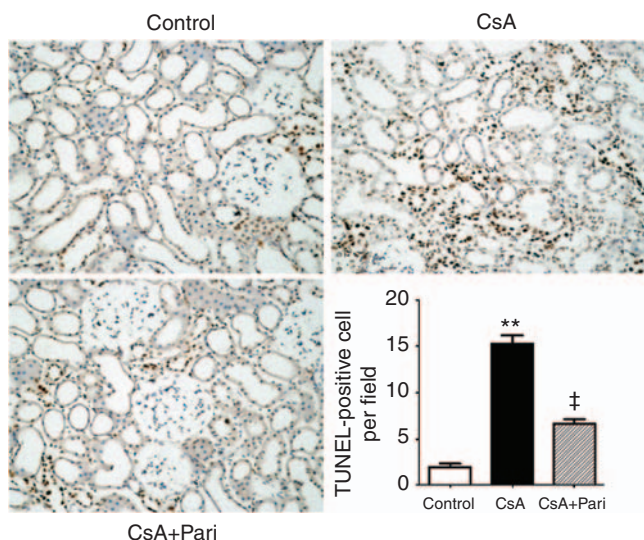


Figure 9 | Effects of CsA treatment on tubular cell apoptosis in rats. The terminal deoxynucleotidyl transferase-mediated dUTP nick end-labeling (TUNEL) assay revealed increased apoptosis in response to cyclosporine (CsA), whereas paricalcitol (Pari) co-treatment significantly reduced the number of TUNEL-positive cells (original magnification, × 100) (*n* = 5 for each group). ***P* < 0.01 compared to the control. †*P* < 0.01 compared to CsA-treated rats.

assess the histological tissue injury. Tubulointerstitial lesion indexes were determined using a semiquantitative scoring system.³¹ Ten fields per kidney were examined by the pathologists, and lesions were graded from 0 to 3 (0, no change; 1, changes affecting < 25% of the section; 2, changes affecting 25–50% of the section; and 3, changes affecting 50–100% of the section), according to the area with tubulointerstitial lesions (tubular atrophy, interstitial inflammation, and fibrosis). The score index in each rat was expressed as a mean value of all scores obtained. We also performed vimentin, a marker of actin microfilament and Masson’s trichrome to visualize ECM accumulation and fibrosis. Masson’s trichrome staining was quantified by image analysis (Scion Image for Windows, Scion Corporation, Frederick, MD, USA) by the pathologists.³² Randomly selected fields (12 per section) were digitized and subjected to color

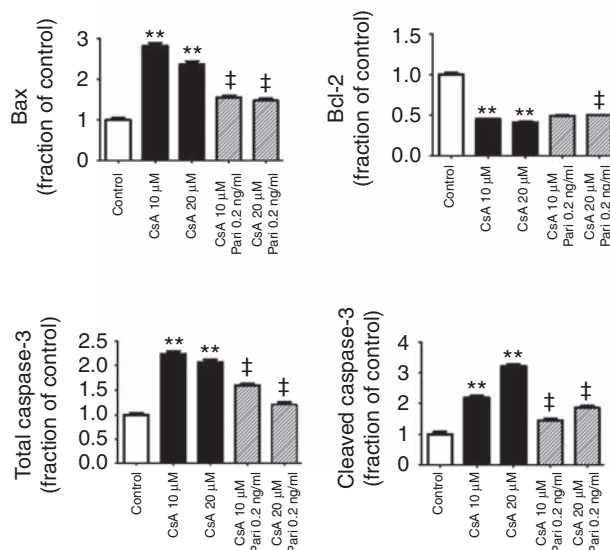
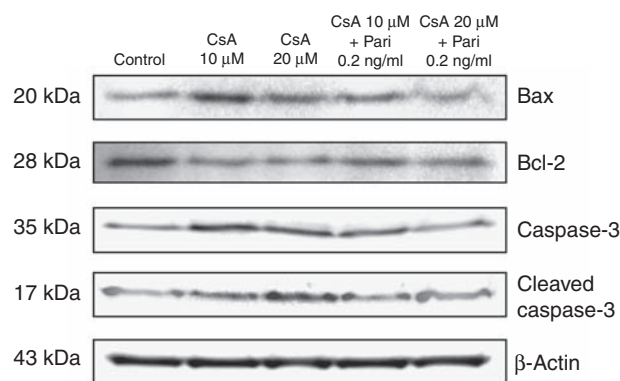


Figure 10 | Effects of paricalcitol on the expression of pro- and anti-apoptotic markers. Semiquantitative immunoblotting indicated that the level of pro-apoptotic marker Bax increased in CsA-treated HK-2 cells, whereas that of anti-apoptotic protein Bcl-2 decreased. Significant increases in total and cleaved caspase-3 expression were noted in CsA-treated cells. Paricalcitol also attenuated all of these changes. CsA, cyclosporine; Pari, paricalcitol. Each column represents the mean ± s.e.m. of three independent experiments performed in duplicate. ***P* < 0.01 compared to the control. †*P* < 0.01 compared to CsA-treated HK-2 cells.

threshold analysis, giving a final average percentage positive stain per section. Immunoperoxidase labeling was performed as described previously.³³

Semiquantitative immunoblotting

The dissected cortex/OSOM was homogenized in ice-cold isolation solution containing 0.3 mol/l sucrose, 25 mmol/l imidazole, 1 mmol/l EDTA, 8.5 μmol/l leupeptin, and 1 mmol/l phenylmethylsulfonyl fluoride (pH 7.2). The homogenates were centrifuged at 1000 × *g* for 15 min at 4 °C to remove whole cells, nuclei, and mitochondria. The total protein concentration was measured. All samples were adjusted with isolation solution to reach the same final protein concentrations and solubilized at 65 °C for 15 min in sodium dodecyl sulfate (SDS)-containing sample buffer and then stored at –20 °C. To confirm equal loading of protein, we stained an initial gel with Coomassie blue. SDS–polyacrylamide gel electrophoresis was performed on 9 or 12% polyacrylamide gels. The proteins were

transferred electrophoretically (Bio-Rad Mini Protean II; Bio-Rad, Hercules, CA, USA) onto nitrocellulose membranes (Hybond ECL RPN3032D; Amersham Pharmacia Biotech, Little Chalfont, UK). The blots were blocked with 5% milk in PBS-T (80 mmol/l Na₂HPO₄, 20 mmol/l NaH₂PO₄, 100 mmol/l NaCl, and 0.1% Tween 20 (pH 7.5)) for 1 h and then incubated overnight at 4 °C with primary antibodies, followed by incubation with secondary anti-rabbit, anti-mouse, or anti-goat horseradish peroxidase-conjugated antibodies. Labeling was visualized using an enhanced chemiluminescence system.

Primary antibodies

The antibodies used were as follows: affinity-purified anti-mouse antibodies against ED-1 (Santa Cruz Biotechnology, Santa Cruz, CA, USA), iNOS (BD Transduction Laboratories, San Jose, CA, USA), E-cadherin (BD Transduction), α -SMA (Sigma Chemical), and fibronectin (Santa Cruz Biotechnology); and anti-rabbit antibodies against phospho-NF- κ B p65 (P-p65; Cell Signaling Technology, Beverly, MA, USA), I κ B- α (Santa Cruz Biotechnology), TGF- β 1 (Santa Cruz Biotechnology), Smad-2/3 (Cell Signaling Technology), Smad-4 (Cell Signaling Technology), Smad-6 (Cell Signaling Technology), pERK 1/2 (Cell Signaling Technology), Bax (Cell Signaling Technology), Bcl-2 (Cell Signaling Technology), total caspase-3 (Cell Signaling Technology), cleaved caspase-3 (Cell Signaling Technology); and anti-goat antibody against vimentin (Santa Cruz Biotechnology) and CTGF (Santa Cruz Biotechnology).

Real-time PCR

The renal cortex was homogenized in TRIzol reagent (Invitrogen, Carlsbad, CA, USA). RNA was extracted with chloroform, precipitated with isopropanol, washed with 75% ethanol, and then dissolved in distilled water. The mRNA expression of inflammatory cytokines and adhesion molecules was determined by real-time PCR. First-strand cDNA was made by reverse transcribing 5 μ g aliquots of total RNA using oligo(dT) primers and Superscript reverse transcriptase II (Invitrogen). Then, cDNA was quantified using the Smart Cycler II System (Cepheid, Sunnyvale, CA, USA) and SYBR Green was used for detection. PCR was performed with 10 μ mol/l forward primer, 10 μ mol/l reverse primer, 2 \times SYBR Green Premix Ex Taq (Takara Bio, Seta, Japan), 0.5 μ l of cDNA, and H₂O to bring the final volume to 20 μ l. Relative levels of mRNA were determined by real-time PCR, using a Rotor-Gene 3000 Detector System (Corbett Research, New South Wales, Australia). The sequences of primers are listed in Table 2.

PCR was performed according to the following steps: (1) 95 °C for 5 min; (2) 95 °C for 20 s; (3) 58–62 °C for 20 s (optimized for each primer pair); (4) 72 °C for 30 s; and (5) 85 °C for 6 s to detect SYBR Green. Steps 2–5 were repeated for an additional 64 cycles. At the end of the last cycle, the temperature was increased from 60 to 95 °C to produce a melting curve. Data from the reaction were collected and analyzed with the appropriate software package from Corbett Research. The comparative critical threshold (Ct) values from quadruplicate measurements were used to calculate the gene expression, with normalization against glyceraldehyde 3-phosphate dehydrogenase as an internal control.³⁴ Melting curve analysis was performed to enhance the specificity of the amplification reaction.

TUNEL assay

Apoptosis was assessed using the TUNEL assay and the numbers of apoptotic cells, as defined by chromatin condensation or nuclear

Table 2 | Primer sequences for real-time PCR

Gene	Sequence	Size (bp)
TNF- α	Fwd: CTTGAGTCCACAGAGAAGAAGTGC	298
	Rev: CACGATCATGTTGGACAAGTCTCC	
IL-1 β	Fwd: TGATGTTCCATTAGACAGC	378
	Rev: GAGGTGCTGATGTACCAGTT	
IFN- γ	Fwd: AACCAGGCCATCAGCAACAACA	214
	Rev: ACCGACTCCTTTCCGCTTCT	
MCP-1	Fwd: AGCCAGAAACCAGCCAAGTCT	196
	Rev: GCCGACTCATTGGGATCATCTT	
ICAM-1	Fwd: GCCCGGAGGATCACAAACGAC	186
	Rev: CCTGGGGCTGGCATGTAAGAGT	
VCAM-1	Fwd: GGGGGCCAAGTCCGTTCTGA	158
	Rev: GGGGGCCACTGAATTGAATCTC	
GAPDH	Fwd: GCCAAAAGGGTTCATCATCTC	229
	Rev: GGCCATCCACAGTCTTCT	

Abbreviations: Fwd, forward; GAPDH, glyceraldehyde 3-phosphate dehydrogenase; ICAM, intercellular adhesion molecule; IFN, interferon; IL, interleukin; MCP, monocyte chemoattractant protein; Rev, reverse; TNF, tumor necrosis factor; VCAM, vascular cell adhesion molecule.

fragmentation, were counted. Apoptosis was detected in the specimen using the ApopTag Plus Peroxidase *In Situ* Apoptosis Detection Kit (Chemicon, Temecula, CA, USA) according to the manufacturer's protocol. TUNEL-positive cells were counted in the cortical tubular cells in ten \times 100 fields per slide.

Statistical analysis

Results are expressed as the mean \pm standard error of the mean (s.e.m.). Multiple comparisons among three groups (control, CsA alone, and CsA + Pari) were performed using one-way analysis of variance and the *post hoc* Tukey's honestly significant difference test. In another experiment for control and paricalcitol alone groups, we use the independent *t*-test to compare the variables. Differences with values of $P < 0.05$ were considered significant.

DISCLOSURE

All the authors declared no competing interests.

ACKNOWLEDGMENTS

This research was supported by Basic Science Research Program through the National Research Foundation (NRF) funded by the Ministry of Education, Science and Technology (2009-0072726), by a grant of the Korea Healthcare Technology R&D Project, Ministry for Health, Welfare & Family Affairs, Republic of Korea (A084869), and by a grant of the Chonnam National University Hospital Research Institute of Clinical Medicine (CRI09026-1).

SUPPLEMENTARY MATERIAL

Table S1. Changes in renal functional parameters.

Figure S1. Changes in inflammatory cytokines in rats treated with paricalcitol alone.

Figure S2. Semiquantitative immunoblotting analysis in rats and HK-2 cells treated with paricalcitol alone compared to controls.

Supplementary material is linked to the online version of the paper at <http://www.nature.com/ki>

REFERENCES

- Kuhlmann A, Haas CS, Gross ML et al. 1,25-Dihydroxyvitamin D₃ decreases podocyte loss and podocyte hypertrophy in the subtotaly nephrectomized rat. *Am J Physiol Renal Physiol* 2004; **286**: F526–F533.
- Makibayashi K, Tatematsu M, Hirata M et al. A vitamin D analog ameliorates glomerular injury on rat glomerulonephritis. *Am J Pathol* 2001; **158**: 1733–1741.

3. Olesen ET, de Seigneux S, Wang G *et al.* Rapid and segmental specific dysregulation of AQP2, S256-pAQP2 and renal sodium transporters in rats with LPS-induced endotoxaemia. *Nephrol Dial Transplant* 2009; **24**: 2338–2349.
4. Brown AJ, Dusso A, Slatopolsky E. Vitamin D. *Am J Physiol Renal Physiol* 1999; **277**: 157–175.
5. Tan X, Li Y, Liu Y. Therapeutic role and potential mechanisms of active Vitamin D in renal interstitial fibrosis. *J Steroid Biochem Mol Biol* 2007; **103**: 491–496.
6. Li Y, Spataro BC, Yang J *et al.* 1,25-Dihydroxyvitamin D inhibits renal interstitial myofibroblast activation by inducing hepatocyte growth factor expression. *Kidney Int* 2005; **68**: 1500–1510.
7. Drüeke TB. Which vitamin D derivative to prescribe for renal patients. *Curr Opin Nephrol Hypertens* 2005; **14**: 343–349.
8. Tan X, Li Y, Liu Y. Paricalcitol attenuates renal interstitial fibrosis in obstructive nephropathy. *J Am Soc Nephrol* 2006; **17**: 3382–3393.
9. Tan X, Wen X, Liu Y. Paricalcitol inhibits renal inflammation by promoting vitamin D receptor-mediated sequestration of NF-kappaB signaling. *J Am Soc Nephrol* 2008; **19**: 1741–1752.
10. Mizobuchi M, Morrissey J, Finch JL *et al.* Combination therapy with an angiotensin converting enzyme inhibitor and a vitamin D analog suppresses the progression of renal insufficiency in uremic rats. *J Am Soc Nephrol* 2007; **18**: 1796–1806.
11. Myers BD, Ross J, Newton L *et al.* Cyclosporine-associated chronic nephropathy. *N Engl J Med* 1984; **311**: 699–705.
12. Chapman JR, Nankivell BJ. Nephrotoxicity of cyclosporin A: short-term gain, long-term pain? *Nephrol Dial Transplant* 2006; **21**: 2060–2063.
13. Wang C, Salahudeen AK. Lipid peroxidation accompanies cyclosporine nephrotoxicity: effects of vitamin E. *Kidney Int* 1995; **47**: 927–934.
14. Naesens M, Kuypers DR, Sarwal M. Calcineurin inhibitor nephrotoxicity. *Clin J Am Soc Nephrol* 2009; **4**: 481–508.
15. Johnson DW, Saunders HJ, Johnson FJ *et al.* Cyclosporin exerts a direct fibrogenic effect on human tubulointerstitial cells: roles of insulin-like growth factor I, transforming growth factor beta1, and platelet-derived growth factor. *J Pharmacol Exp Ther* 1999; **289**: 535–542.
16. Vieira Jr JM, Noronha IL, Malheiros DM *et al.* Cyclosporine-induced interstitial fibrosis and arteriolar TGF-beta expression with preserved renal blood flow. *Transplantation* 1999; **68**: 1746–1753.
17. Miyajima A, Chen J, Lawrence C *et al.* Antibody to transforming growth factor-beta ameliorates tubular apoptosis in unilateral ureteral obstruction. *Kidney Int* 2000; **58**: 2301–2313.
18. Li C, Yang CW, Park JH *et al.* Pravastatin treatment attenuates interstitial inflammation and fibrosis in a rat model of chronic cyclosporine-induced nephropathy. *Am J Physiol Renal Physiol* 2004; **286**: F46–F57.
19. Lee SH, Li C, Lim SW *et al.* Attenuation of interstitial inflammation and fibrosis by recombinant human erythropoietin in chronic cyclosporine nephropathy. *Am J Nephrol* 2005; **25**: 64–76.
20. Buffoli B, Pechánová O, Kojsová S *et al.* Provilin prevents CsA-induced nephrotoxicity by reducing reactive oxygen species, iNOS, and NF-kB expression. *J Histochem Cytochem* 2005; **53**: 1459–1468.
21. Magendiramani V, Umesalma S, Kalayarasan S *et al.* S-allylcysteine attenuates renal injury by altering the expressions of iNOS and matrix metallo proteinase-2 during cyclosporine-induced nephrotoxicity in Wistar rats. *J Appl Toxicol* 2009; **29**: 522–530.
22. Liu Y. Epithelial to mesenchymal transition in renal fibrogenesis: pathologic significance, molecular mechanism, and therapeutic intervention. *J Am Soc Nephrol* 2004; **15**: 1–12.
23. Böttinger EP, Bitzer M. TGF-beta signaling in renal disease. *J Am Soc Nephrol* 2002; **13**: 2600–2610.
24. Akool el-S, Doller A, Babelova A *et al.* Molecular mechanisms of TGF beta receptor-triggered signaling cascades rapidly induced by the calcineurin inhibitors cyclosporin A and FK506. *J Immunol* 2008; **181**: 2831–2845.
25. Cantley LC. The phosphoinositide 3-kinase pathway. *Science* 2002; **296**: 1255–1267.
26. Masaki T, Foti R, Hill PA *et al.* Activation of the ERK pathway precedes tubular proliferation in the obstructed rat kidney. *Kidney Int* 2003; **63**: 1256–1264.
27. Chan ED, Riches DW. IFN-gamma + LPS induction of iNOS is modulated by ERK, JNK/SAPK, and p38(mapk) in a mouse macrophage cell line. *Am J Physiol Cell Physiol* 2001; **280**: C441–C450.
28. Ma FY, Flanc RS, Tesch GH *et al.* A pathogenic role for c-Jun amino-terminal kinase signaling in renal fibrosis and tubular cell apoptosis. *J Am Soc Nephrol* 2007; **18**: 472–484.
29. Yang CW, Faulkner GR, Wahba IM *et al.* Expression of apoptosis-related genes in chronic cyclosporine nephrotoxicity in mice. *Am J Transplant* 2002; **2**: 391–399.
30. Sanz AB, Santamaría B, Ruiz-Ortega M *et al.* Mechanisms of renal apoptosis in health and disease. *J Am Soc Nephrol* 2008; **19**: 1634–1642.
31. Gadola L, Noboa O, Marquez MN *et al.* Calcium citrate ameliorates the progression of chronic renal injury. *Kidney Int* 2004; **65**: 1224–1230.
32. Oldroyd SD, Miyamoto Y, Moir A *et al.* An IGF-I antagonist does not inhibit renal fibrosis in the rat following subtotal nephrectomy. *Am J Physiol Renal Physiol* 2006; **290**: F695–F702.
33. Kim SW, Wang W, Nielsen J *et al.* Increased expression and apical targeting of renal ENaC subunits in puromycin aminonucleoside-induced nephrotic syndrome in rats. *Am J Physiol Renal Physiol* 2004; **286**: F922–F935.
34. Livak KJ, Schmittgen TD. Analysis of relative gene expression data using real-time quantitative PCR and the 2(-Delta Delta C(T)) Method. *Methods* 2001; **25**: 402–408.